

# Hybrid electric buses fuel consumption prediction based on real-world driving data

Ruixiao Sun<sup>1</sup>, Yuche Chen<sup>1\*</sup>, Abhishek Dubey<sup>2</sup>, Philip Pugliese<sup>3</sup>

<sup>1</sup>Department of Civil and Environmental Engineering, University of South Carolina, Columbia, SC 29209

<sup>2</sup>Department of Electric Engineering and Computer Science, Vanderbilt University, Nashville, TN 37203

<sup>3</sup>Chattanooga Area Regional Transportation Authority, 1617 Wilcox Boulevard, Chattanooga, TN 37406

\* Corresponding author: Yuche Chen, [chenyuc@cec.sc.edu](mailto:chenyuc@cec.sc.edu)

## Abstract

Estimating fuel consumption by hybrid diesel buses is challenging due to its diversified operations and driving cycles. In this study, long-term transit bus monitoring data were utilized to empirically compare fuel consumption of diesel and hybrid buses under various driving conditions. Artificial neural network (ANN) based high-fidelity microscopic (1Hz) and mesoscopic (5-60 minutes) fuel consumption models were developed for hybrid buses. The microscopic model contained 1 Hz driving, grade, and environment variables. The mesoscopic model aggregated 1Hz data into 5 to 60-minute traffic pattern factors and predicted average fuel consumption over its duration. The prediction results show mean absolute percentage errors of 1-2% for microscopic models and 5-8% for mesoscopic models. The data were partitioned by different driving speeds, vehicle engine demand, and road grade to investigate their impacts on prediction performance.

**Keywords:** hybrid diesel transit bus; artificial neural network; fuel consumption prediction

## 1. Introduction

Globally, the transportation sector consumes 83 trillion megajoules of energy and produces 5.7 gigatons of greenhouse gas (GHG) emissions, along with other criteria pollutants, that contribute to 200,000 annual premature deaths (Frey, 2018). Public transportation may potentially reduce energy consumption by conveying larger passenger volumes in less space than private automobiles (White, 2016). Emerging technologies, including automation, internet of things, and the sharing economy enable innovations in transit operations, which provide greater potential in achieving sustainability goals in the transportation sector (Shen et al., 2018). However, public transportation service has high operational and capital costs due to its low occupancy rate. For example, in United States, the average operating and capital costs of the nation's 10 largest bus systems are \$0.85 and \$0.16 per passenger mile, which are substantially higher than those of private automobiles, which are \$0.11 and \$0.14 per passenger mile<sup>1</sup>. According to United States Bureau of Transportation Statistics, fuel cost is approximately 20 percent of total transit operating costs (BTS, 2018). The non-plug-in electric hybrid bus has attracted attention from transit authorities, and its market share has been steadily increasing over the past decade (DOE, 2019). For brevity, the non-plug-in electric hybrid bus is referred to as the hybrid electric bus in this paper. A hybrid bus has a small battery and an electric motor on board, which can provide supplemental propulsion, particularly at low speeds with heavy traffic and frequent stop-and-go driving. Thus, changes in fuel consumption of a hybrid bus, as compared with conventional diesel buses, depend on the driving cycle, driving behavior, and energy management of the hybrid bus. Clark et al. (2009) showed improvements to fuel economy ranging from 16% to 48% for hybrid buses, when compared to diesel buses, based on different driving cycles. Therefore, to implement energy-saving operation of transit buses, accurate prediction models are needed to understand the fuel consumption behavior of hybrid buses. However, there is currently a knowledge gap regarding this understanding in the literature.

### 1.1 Literature review

In the literature, methodologies to estimate the fuel consumption of transit buses can be divided into summary or estimation models. Summary models focus on comparing trip or daily average

---

<sup>1</sup> The data is obtained from the website [http://www.portlandfacts.com/cost\\_of\\_transit\\_&\\_cars.html](http://www.portlandfacts.com/cost_of_transit_&_cars.html), accessed on September 28<sup>th</sup>, 2020.

fuel consumption of transit buses based on in-use or simulated data. [Zhang et al. \(2014\)](#) and [Wu et al. \(2015\)](#) tested several types of buses, including conventional diesel, natural gas, and diesel hybrid, in Beijing and Macao, using portable emission measurement systems (PEMS). They found that hybrid diesel buses can achieve reductions of 18-29% in fuel consumption. Though not studying hybrid buses, [Holmén and Sentoff \(2015\)](#) is one of the few studies that compares the fuel consumption of a hybrid electric passenger car to an internal combustion car with the same chassis under real-world driving, and they defined a “benefit” factor of the hybrid car for each vehicle specific power bin. In addition to laboratory tests, some researchers summarized the fuel benefits of hybrid electric buses using the simulation-based method ([Lajunen, 2014](#); [Taymaz and Benli, 2014](#)). [Choi and Frey \(2010\)](#) developed a methodology that provided comparisons of high-resolution fuel use and emission characterization of a hybrid diesel school bus and a conventional diesel bus. They summarized fuel use and benefits of hybrid buses under five driving cycles. They found that the hybrid bus provided large fuel benefits on arterial routes but fewer benefits on highway or local routes. While this study is relevant, it was conducted approximately 10 years ago, and recent technologies must be incorporated in assessments of the fuel benefits of hybrid buses. Additionally, these summary models do not explore statistical relationships between fuel consumption and influencing variables but rather depend on a large number of measurements to ensure statistically robust results.

Estimation models refer to fuel consumption predictions of transit buses using different types of statistical models and with different degrees of granularity. Linear or nonlinear regression-based prediction methodologies are most popular in the literature, particularly for diesel bus fuel estimation. [Tang et al. \(2016\)](#) and [López-Martínez et al. \(2017\)](#) adopted a regression model with categorical, independent variables based on time of day, time of week, and road type to predict fuel rate of buses in different countries. [Wang and Rakha \(2017\)](#) developed quadratic format fuel consumption models for diesel and hybrid buses. They found that buses achieved their lowest rate of fuel consumption when they were cruising at speeds between 39 to 47 km/h within grades of 0-8%. The rate of fuel consumption increased with higher grade and load. Some studies developed advanced and machine learning-based models. Advanced prediction methods, such as neural network or support vector machine, have been used in the literature to predict fuel and emissions

of diesel buses (Wang et al., 2018; Zeng et al., 2015), but few studies have focused on hybrid buses.

## 1.2 Contribution of the work

The literature review demonstrates a need to develop fuel consumption estimation models for hybrid buses based on long-term, in-use experiment data. A high-resolution fuel prediction model for hybrid diesel buses can enable transit operators to improve their planning and bus operations to achieve their fuel savings and sustainability goals. In this study, we propose artificial neural network (ANN) based fuel consumption estimation models that utilize real-world operation data with 1Hz granularity to achieve accurate predictions of microscopic and mesoscopic fuel consumption of hybrid diesel buses. Specifically, the microscopic model utilizes second-level vehicle trajectories to predict fuel consumption rate of hybrid diesel buses at 1Hz frequency. The mesoscopic model estimates average fuel consumption rate at 5, 15, 30, and 60-minute durations based on aggregated traffic pattern factors. In addition, fuel consumption differences between hybrid and diesel buses and potential influencing factors are assessed. We acknowledge that the developed model and estimation coefficients obtained in this study are specific to the studied fleet and region. However, the ANN estimation model framework is applicable to different fleets in other regions if similar transit bus measurement data are available.

## 2. Material and Methods

### 2.1 Experiment Setup and Input data

The data used in this study are 1Hz driving and fuel consumption measurements recorded by on-board sensors on one diesel transit bus and one hybrid non-plug-in electric transit bus between March 2019 and March 2020. The buses are in the transit operating fleet of the Chattanooga Area Regional Transportation Authority (CARTA). They were manufactured by Gillig Brothers Inc. Table 1 summarizes the specifications of the diesel and hybrid buses.

**Table 1. Chassis and Engine Information for Gillig Model Year 2014 Diesel and Hybrid Buses**

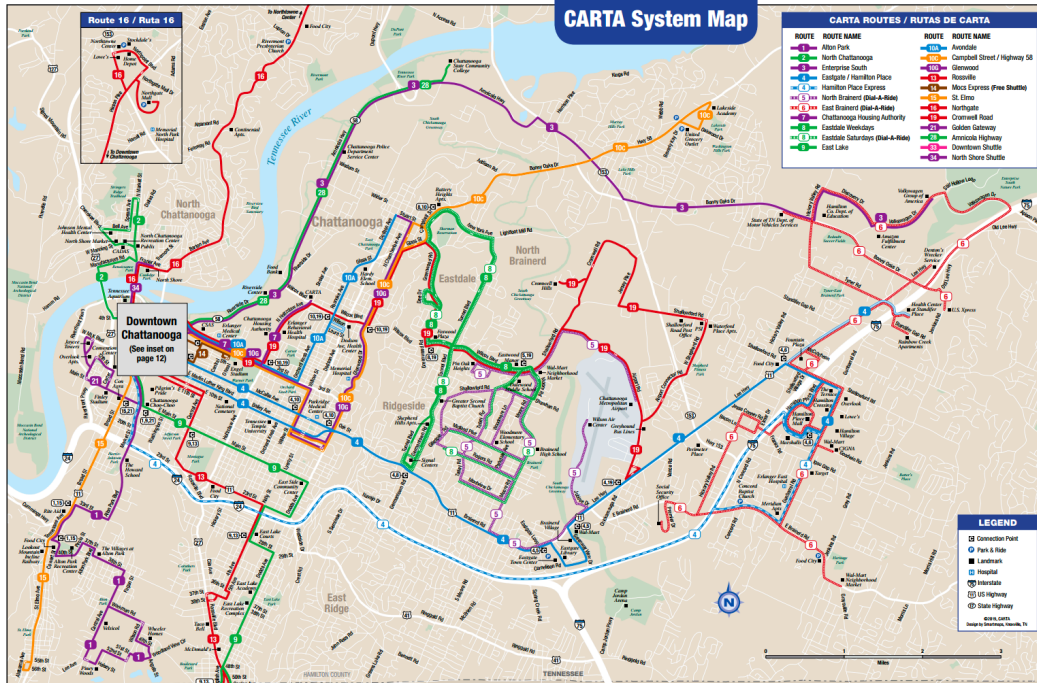
Characteristic	Diesel Bus	Hybrid Bus
<b>Seat Capacity</b>	32 seats	32 seats
<b>Model year</b>	2014	2014
<b>Hybrid architecture</b>	N/A	Parallel
<b>Powertrain</b>	Engine: Cummins ISL	Engine: Cummins ISB

		Motor: Allison H40EP
<b>Powertrain Power</b>	264 kW	261 Kw (209 kW for engine)
<b>Energy Storage System Weight</b>	N/A	440 kg
<b>Curb weight</b>	11,600 kg	12,400 kg

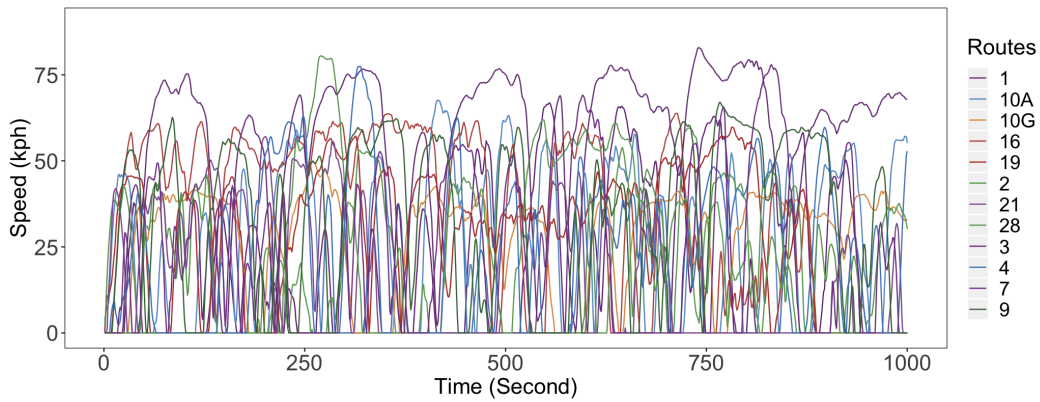
The collected data were 1Hz frequency real-time location coordinates (i.e. latitude, longitude), elevation, ambient temperature, vehicle dynamics (instantaneous speed and acceleration), and fuel consumption rate. Data on vehicle dynamics and fuel consumption were obtained by gathering information with the vehicle’s control area network bus (CAN bus) using a data logger called Datahub developed by ViriCiti Inc<sup>2</sup>, which complies with the Society of Automotive Engineers J1939 standard. The data logger contained an accelerometer to measure instantaneous speed and transform the location to longitude and latitude coordinates. The temperature was obtained through query Dark Sky API weather data<sup>3</sup>. The elevation data were queried through elevation databases according to instantaneous bus coordinates. The elevation database was provided by the Tennessee elevation LiDAR project, which is a coordinated effort with the United States Geological Survey. The Tennessee Elevation LiDAR database provides elevation data and the majority of GPS locations (with 1-2 foot contour) in State of Tennessee (TN, 2020). Based on the elevation data, the road grade of each 1Hz measurement is calculated by dividing the elevation difference between current and previous measurements by the driving distance. We have to acknowledge that there are limitations on using geographic information system data to calculate road grade, because road grade normally does not match the general slope of the land. Particularly, major roads are constructed to reduce grade if the terrain is hilly. We use the road grade data based on Tennessee Elevation LiDAR database, but will look for better road grade data if they are available. The driving data are collected from transit buses running on all routes operated by CARTA, as shown in Figure 1 (a), and typical driving trajectory for each route is presented in Figure (b). The routes represent typical mountainous terrain patterns in the region, which is surrounded by the Tennessee River and the ridge-and-valley Appalachians. The driving cycles have speeds up to 40-50 kph and an acceleration range of -2 to 2 meter per second.

<sup>2</sup> ViriCiti Inc. DataHub. <https://viriciti.com/datahub/>

<sup>3</sup> Dark Sky Weather API. <https://darksky.net/dev/docs>



(a)



(b)

Route	Length (km)	Route	Length (km)	Route	Length (km)
1	10.3	10a	14.6	16	23.2
2	10.6	10c	29.0	19	38.9
4	19.1	10g	9.5	21	8.4
7	5.6	13	12.6	28	26.1
8	8.7	14	9.3	33	3.9
9	17.7	15	10.1		

(c)

Figure 1. Route map (a), typical driving trajectories for bus routes (b), and route length (c) of Chattanooga Area Regional Transportation Authority (CARTA, 2020).

### 3 Comparison of fuel consumption of hybrid and conventional diesel buses

In Figure 2, the distribution of amount of time spent in vehicle specific power (VSP), speed, and road grade bins for diesel and hybrid buses are compared. VSP is an evaluation metric for vehicle energy consumption and emissions. As stated in Jimenez-Palacios (1998), “it is the sum of loads resulting from aerodynamic drag, acceleration, rolling resistance, and hill climbing, all divided by the mass of the vehicle”. VSP is calculated by dividing the instantaneous power for kinetic, potential, rolling, and aerodynamic resistance by vehicle weight,

$$VSP = \frac{\frac{d}{dt}(KE + PE) + F_{rolling} * v + F_{Aerodynamic} * v}{m} = \frac{\frac{d}{dt}(\frac{1}{2}m * (1 + \epsilon_i) * v^2 + m * g * h) + C_R * m * g * v + \frac{1}{2}\rho * C_D A v^3}{m}$$

$$= v * (a * (1 + \epsilon_i) + g * grade + g * C_R) + \frac{1}{2}\rho \frac{C_D A}{m} v^3$$

The unit for VSP is kW per ton. VSP is considered to be a surrogate measurement for the instantaneous power demand of a vehicle normalized to its own weight and has been used in recent literature (Chen et al., 2017; Frey et al., 2007). Figure 2 show similarities in driving status and road grade conditions for the diesel and hybrid buses.

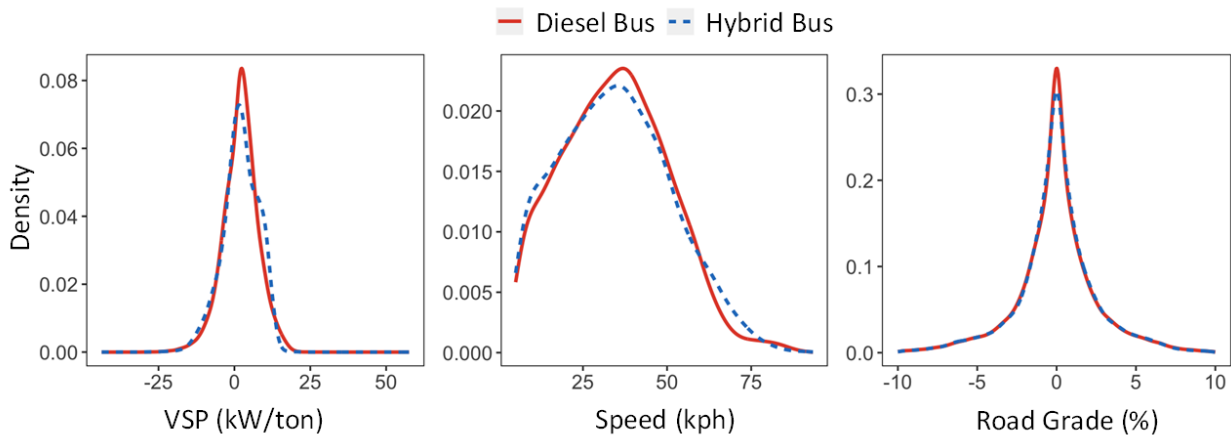


**Figure 2. Vehicle specific power, speed and road grade distribution comparison of diesel and hybrid driving.**

Figure 3 shows the average fuel consumption rates of diesel and hybrid buses as a function of instantaneous VSP with 1kW/ton interval. VSP measures a vehicle’s tractive power normalized to its own weight. Thus, the comparison in Figure 3 accounts for the difference in the weight of hybrid and diesel buses. Each average fuel consumption rate was averaged over at least 2,000 instantaneous measurements to ensure statistical robustness. The results show a positive relationship between VSP and the bus fuel consumption rate. However, the slope of the curves decreases when VSP is greater than 15 kW/ton. This observation is expected and is consistent with

previous studies (Wang and Rakha, 2016; Zhang and Yao, 2015). Similar patterns of fuel savings for hybrid buses were observed in other studies (Wayne et al., 2004; Wu et al., 2014).

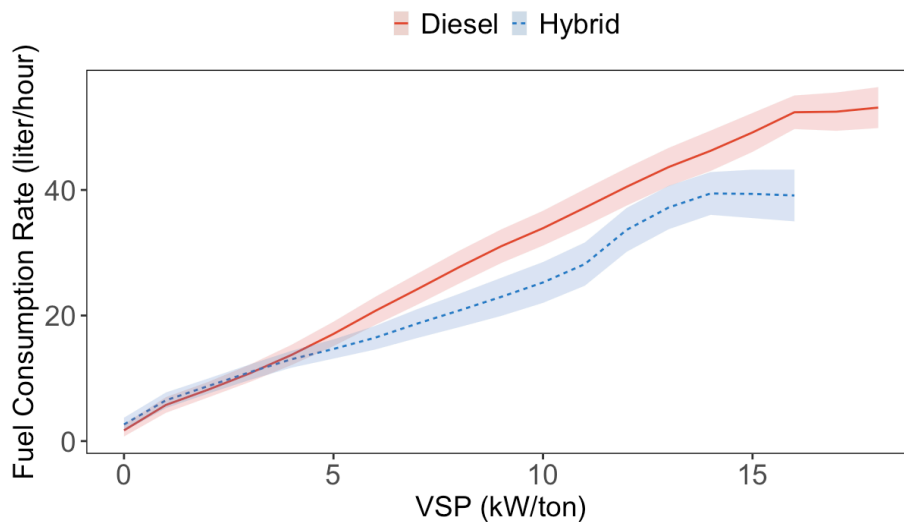


**Figure 3. Mean fuel rate (liter per hour) and 95% confidence interval (shaded area) for diesel and hybrid bus as a function of instantaneous vehicle specific power bins from 0 to 18 kW/ton with 1 kW/ton interval.**

Figure 4 reports the percentage of fuel savings for hybrid buses compared with diesel buses, accounting for driving speed and VSP. The results are controlled in three speed categories: 1) 1 to 40 kph (equivalent to 25 miles per hour), 2) 40 to 80 kph (equivalent to 50 miles per hour), and 3) above 80 kph. These three categories correspond to typical local, arterial, and highway driving conditions. This categorization is consistent with that used in MOVES, a widely used model for vehicle energy and emission analysis (US EPA, 2010). Figure 4 shows that the fuel benefits of hybrid buses vary, depending on driving conditions. For local driving (speeds up to 40 kph), the fuel savings for hybrid buses increase linearly as the VSP increases. The fuel savings could be as little as 0% at low VSP (5 kW/ton) or as high as 70% at high VSP (17 kW/ton). In local driving, the high VSP typically represents aggressive acceleration from stop or low speeds during heavy traffic or from bus stops. Under arterial driving conditions (speeds between 40 and 80 kph), hybrid buses have the same fuel efficiency as the diesel buses until the VSP is greater than 15 kW/ton. At a VSP of 18 kW/ton, the fuel savings are approximately 10%. The high VSP in arterial driving typically corresponds to aggressive acceleration to avoid heavy traffic. For highway driving, the fuel efficiency of hybrid buses is worse than diesel buses when VSP is greater than 5 kW/ton. However, steady highway driving does not appear to account for drivers that are “dithering” the

pedal, which would result in vibrative power demand and create charging opportunities for hybrid buses. Very high-resolution speed data are needed to perceive the “dithering” effect, which may be a direction for future data collection and research. Holmen and Sentoff (2015) found that the fuel consumption for a hybrid gasoline passenger car is 5-20% worse than a comparable gasoline car under highway driving conditions with a VSP greater than 10 kW/ton. Choi and Frey (2010) showed that a parallel hybrid diesel school bus reported 3-9% worse fuel consumption rates than a comparable conventional diesel school bus under highway and arterial driving conditions.

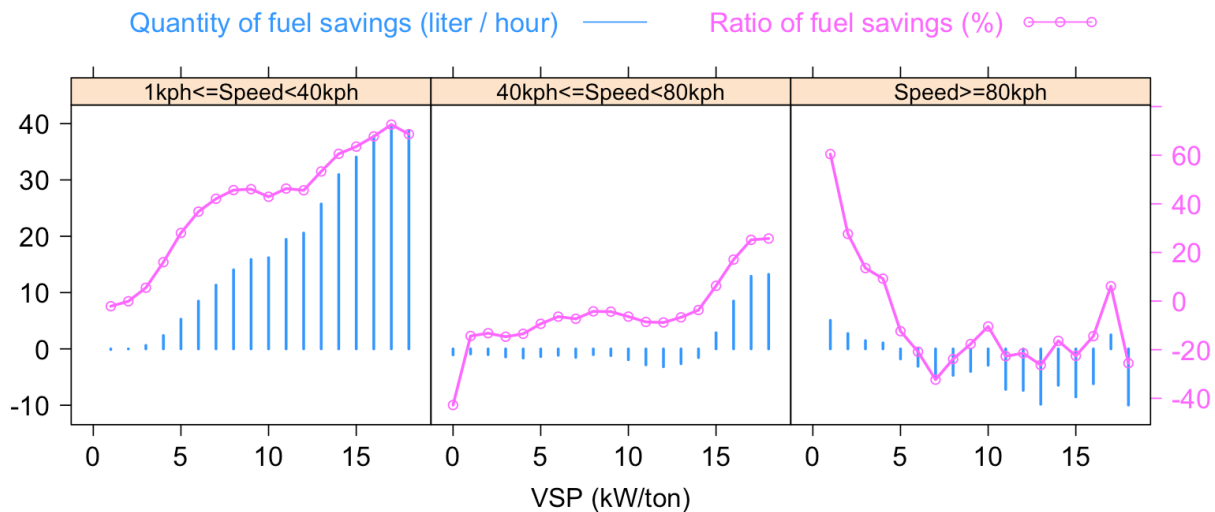


**Figure 4. Fuel savings of hybrid buses as compared with diesel buses by driving speed and instantaneous vehicle specific power bins.**

#### 4 Development of a fuel consumption prediction model

This study aims to develop ANN-based models for predicting fuel consumption rates for hybrid diesel transit buses at the microscopic and mesoscopic levels. In the microscopic model, the fuel rate (liters per hour) is estimated based on velocity, acceleration, and road grade, as well as other vehicle and road characteristics factors at 1Hz frequency. In the mesoscopic model, fuel estimates are based on aggregated traffic pattern information for trip durations of 5, 15, 30, and 60 minutes. As shown in Figure 5, the model development and applications are illustrated in three modules. In the 1<sup>st</sup> module, which is referred to as “data preparation.”, vehicle trajectory and fuel consumption data at 1Hz frequency are collected and processed into 5, 15, 30, or 60-minute trip duration average metrics. In the “model development” module, artificial neural network models are built for 1Hz data and aggregated data at different trip durations to estimate the fuel rates of hybrid buses. In each model, the dataset was divided into datasets of training, validation, and testing. Training data

was used to fit a prediction model. The validation set was used to perform parameter/model selection and to cope with overfitting, which is considered part of the training process. The testing set was used to evaluate model performance. The prediction results were at the same time resolution of the input data, as prepared in “data preparation” module. Finally, in the “model application” module, the developed models can be applied at different time resolutions with various input variables, depending on the specific applications. This approach provided flexibility in model application, particularly given that users have varying degrees of access to the input data.

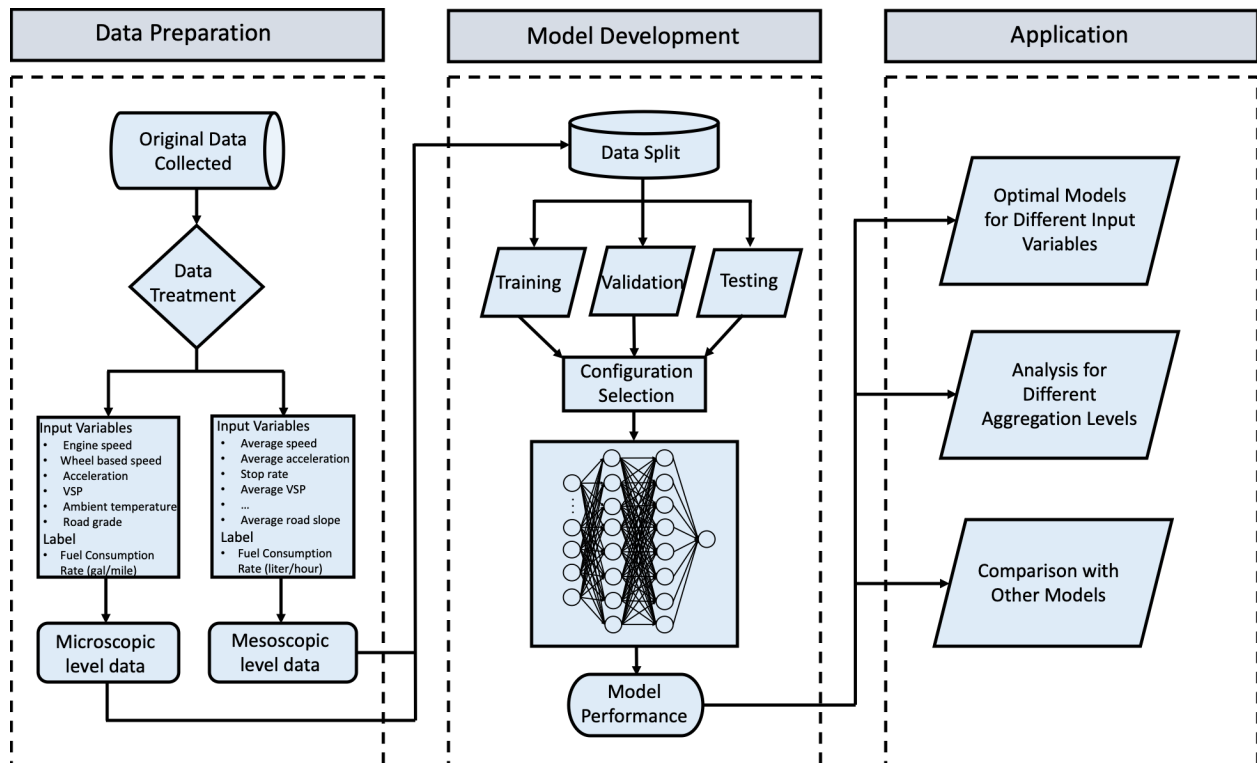


Figure 5. Flowchart of the main tasks

#### 4.1 Data preparation

The microscopic model predicts fuel consumption rate (liters per hour) using vehicle speed/velocity, acceleration, road grade, ambient temperature, and VSP at 1Hz frequency as the input variables. To prepare mesoscopic models, the collected 1Hz data are processed into 11 independent variables and the predicting variable, i.e. fuel consumption rate (liter per 100 kilometer), as shown in Table 2. The ability to capture temperature data was helpful for both microscopic and mesoscopic models to infer fuel consumption used for air conditioning, since all the buses in this study were not equipped with a heating burner. Passenger load can influence the fuel consumption of buses, particularly under heavy load conditions (Liu et al., 2019). However,

passenger load information was not included in the data that was collected for this study. However, obtaining this information may be a future direction for data collection and future research.

**Table 2. Description of mesoscopic model input data**

Symbols	Descriptions
$n$	The index of analysis snippet
$T$	The time span of an analysis snippet (i.e. 5min, 15min, 30min, 60min)
$t$	The index of second in an analysis snippet, $t=\{1, 2, \dots, T\}$
$d_t^n$	The cumulative distance at second $t$ of snippet $n$ (kilometer)
$v_t^n$	The instantaneous speed at second $t$ of snippet $n$ (kilometer / hour)
$f^n$	The cumulative fuel consumed at the end of snippet $n$ (liter)
$\bar{v}^n$	The average speed of snippet $n$ (kilometer / hour)
$v\sigma^n$	The standard deviation of speed in snippet $n$
$\bar{a}^n$	The average acceleration of snippet $n$ (meter / second <sup>2</sup> )
$a_t^n$	The instantaneous acceleration at second $t$ of snippet $n$ (meter / second <sup>2</sup> )
$a\sigma^n$	The standard deviation of acceleration in snippet $n$
$VSP_t^n$	The vehicle specific power at second $t$ of snippet $n$ (kW/Metric Ton)
$l_t^n$	The elevation of vehicle at second $t$ of snippet $n$ (meter)
$g_t^n$	The road grade at second $t$ of snippet $n$ (%)
$g\sigma^n$	Standard deviation of road grade at second level in snippet $n$
$g^n$	The road grade at snippet $n$ (%)
$s_t^n$	The driving status index of a bus at second $t$ of snippet $n$ , 1=moving, otherwise 0
$q^n$	The total number of stop-and-go driving events in snippet $n$
$s^n$	Percentage of time in stop position during snippet $n$
$w_t^n$	The ambient temperature at second $t$ of snippet $n$ (°F)
$r^n$	Average fuel consumption rate in snippet $n$ (liter per 100 kilometer)

- (1) Average speed (kilometer/hour) in snippet  $n$ :  $\bar{v}^n = \frac{d_T^n - d_1^n}{T}, \forall n$ .
- (2) Standard deviation of speed in snippet  $n$ :  $v\sigma^n = \frac{\sqrt{\sum_{t=1}^T (v_t^n - \bar{v}^n)^2}}{T-1}$ .
- (3) Average acceleration (meter/second<sup>2</sup>) in snippet  $n$ :  $\bar{a}^n = \frac{\sum_{t=2}^T (v_t^n - v_{t-1}^n)}{T-1} = \frac{v_T^n - v_1^n}{T-1}$ .
- (4) Standard deviation of acceleration in snippet  $n$ :  $a\sigma^n = \frac{\sqrt{\sum_{t=1}^T (a_t^n - \bar{a}^n)^2}}{T-1}$ .
- (5) Stop-and-go times in snippet  $n$ :  $sg^n = \sum_{t=2}^T |s_t^n - s_{t-1}^n|$ .
- (6) Stop rates in snippet  $n$ :  $s^n = \frac{\sum_{t=1}^T s_t^n}{T}$ .
- (7) Average ambient temperature (°F) in snippet  $n$ :  $\bar{w}^n = \frac{\sum_{t=1}^T w_t^n}{T}$ .

(8) Average road grade at second level in snippet  $n$ :  $\bar{g}^n = \frac{\sum_{t=1}^T g_t^n}{T}$ .

(9) Standard deviation of road grade at second level in snippet  $n$ :  $g\sigma^n = \sqrt{\frac{\sum_{t=1}^T (g_t^n - \bar{g}^n)^2}{T-1}}$ .

(10) Road grade in snippet  $n$ :  $g^n = \frac{l_t^n - l_1^n}{d_t^n - d_1^n}$ .

(11) Average Vehicle Specific Power (VSP) (kW/Metric Ton) in snippet  $n$ :  $\overline{VSP}^n = \frac{\sum_{t=1}^T VSP_t^n}{T}$ ,

where,  $VSP_t^n = v_t^n (1.1a_t^n + 9.81g_t^n + 0.132) + 3.02 \times 10^{-4}(v_t^n)^3$ , with  $v_t^n$  in meter/second and  $a_t^n$  in meter/second<sup>2</sup>, (Jimenez-Palacios, 1998).

(12) Fuel used rate in snippet  $n$ :  $r^n = \frac{f^n - f^{n-1}}{d_t^n - d_1^n}$ ,  $\forall n, f^0 = 0$ .

#### 4.2 Artificial Neural Networks Development

The artificial neural network (ANN) approach was employed to estimate fuel consumption rates using the prepared data. An ANN model processes information in the same way that the human brain processes information (Hassoun, 1995). Specifically, an ANN model contains input, along with hidden and output layers, and each layer contains data processing components called neurons. These neurons or processing components are connected to each other and can form complex nonlinear models through activation functions. The activation function determines the value of the neurons in the next layer or the output, based on values and coefficients of neurons in the current layer. Thus, the ANN model can identify the relationship between input and output variables by exploring different forms and weight combinations of neurons in the input and hidden layers, which makes the ANN model a perfect candidate model to be used in this study. For example, a previous study showed that air conditioning (AC) loads in buses can consume significant amounts of energy (Wayne et al., 2004). However, the measurement data did not include AC auxiliary power. To account for AC loads in fuel consumption, ambient temperature is included as an input variable in the estimation model. The relationship between temperature and fuel consumption of buses is not a linear relationship, but a convex quadratic relationship with higher fuel consumption at high and low ends of the temperature spectrum. Thus, the ANN model is capable of representing complex nonlinear relationships.

The activation function is responsible for transforming the set of neurons in one layer into a given neuron or output in the next layer. There are two major types of activation functions: the nonlinear activation function and the linear activation function. Nonlinear activation functions allow neural

network models to represent complex relationships using only a small number of input variables. Therefore, several major types of nonlinear functions were tested to identify the functions that maximize the predictability of the model. These functions are the sigmoid function  $(\frac{1}{1+e^{-x}})$ , the tanh-sigmoid function  $(\frac{2}{1+e^{-2x}} - 1)$ , and the rectified function  $(\max\{0, x\})$ .

Due to severe computations on the high dimensional data when training the ANN models, it is a common practice to scale input data using normalization,  $x_i = \frac{x_i - \min(x)}{\max(x) - \min(x)}$ , where  $x_i$  is the observation for the parameter, and  $\min(x)$  and  $\max(x)$  are the minimum and maximum observations, respectively. Clearly, the performance of an ANN model depends on its configuration. Selecting more hidden layers may increase the accuracy of the network but can increase training time due to its complexity and may result in overfitting. [Karsoliya \(2012\)](#) proved that a neural network with up to two hidden layers is sufficient to represent complex, nonlinear relationships. Moreover, the experimental results in this paper reveal that the first and second hidden layer should contain an equal number of neurons so that the network can be trained easily. The number of neurons in hidden layers are generally determined by using a trial-and-error method ([Maier and Dandy, 2001](#)). A frequently used upper limit for the number of neurons in a hidden layer is  $N_h \leq 2N_i + 1$ , where  $N_h$  is the number of neurons in the hidden layers, and  $N_i$  is the number of input variables ([Maier and Dandy, 2001](#)). Additionally, [Rogers and Dowla \(1994\)](#) recommend  $N_h \leq \frac{S_t}{N_i + 1}$ , where  $S_t$  is the sample size of the training data, to avoid overfitting. In this study, the minimum of the two  $N_h$  is chosen as the upper limit for the number of hidden layer neurons. To get the best approximation of the hidden layer neurons, the number of neurons can be reduced, and training is done to determine whether the network converges to the same solution.

The measurement data are randomly partitioned into training, validation, and testing datasets as 70%:15%:15% ([Taylor, 2006](#)). Specifically, an ANN model is trained using the training set. Then, before testing for prediction performance, training progress is monitored by using independent data, i.e. the validation set, to measure how well the neural network is generalizing outside of the training set. Only models that satisfy our prediction performance threshold on the validation set will be chosen and used for predictions using the test set.

## 5. Results and discussion

### 5.1. Microscopic model selection and prediction performance

Data that are collected at 1Hz frequency are considered to be independent variables in the microscopic model. These data include engine speed, wheel-based speed, acceleration, road grade, ambient temperature, and VSP. The best model yields a mean absolute percentage error (MAPE) of 36%,  $R^2$  of 0.96, and a mean absolute error (MAE) of 1.5 liters per hour, although there are several model setups that have similar prediction performance metrics. The prediction metrics are calculated by comparing the predicted and actual fuel consumption of each 1Hz record. Then, the results are averaged or aggregated to obtain the metrics. Figure 6 compares actual and estimated fuel consumption rates (liters per hour) at every second for one randomly chosen trip. The results show a general alignment between the actual and estimated fuel consumption rates. However, estimation randomness can lead to larger absolute percentage errors at small (i.e., small denominator when calculating the percentage error) fuel consumption rate occurrences. Therefore, the MAPE of 36% for the 1Hz level prediction is primarily determined by errors at small fuel consumption occurrences.

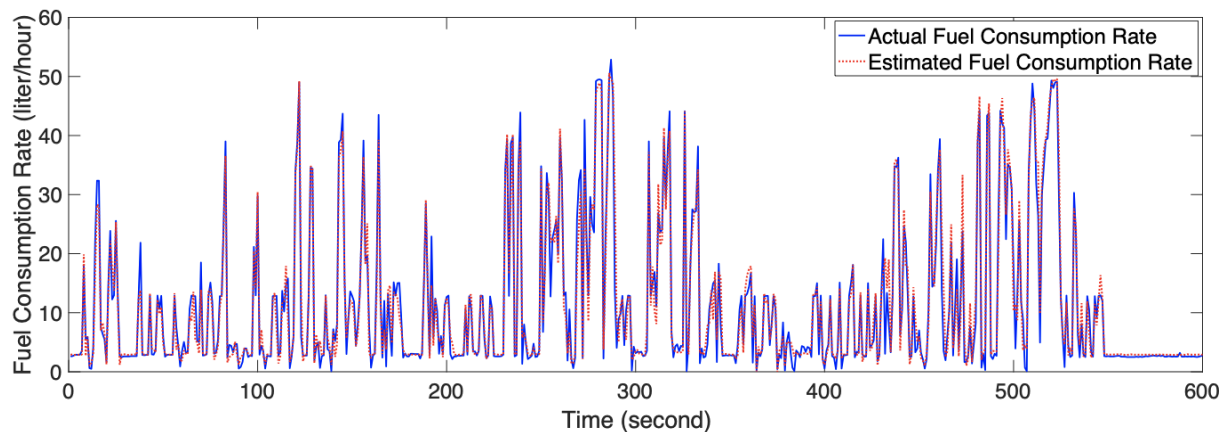


**Figure 6. Second by second actual fuel consumption rate (liter per hour) versus estimated fuel consumption rate for one trip.**

The fuel consumption predictions are accumulated into 5, 15, 30, 60-minute average fuel consumption rates and compared with actual values. We acknowledge that evaluating the microscopic model using cumulative error over a trip could overlook variations in prediction error at the 1Hz level. Since the targeted user scenario of the proposed models is transit operation planning, the focus was on trip level results, although the prediction was done at 1Hz level.

**Table 3. Description of Microscopic level ANNs Configuration Selection Process.**

Hidden layers	Neurons		MAE (liter/hour)	MAPE (%)	R <sup>2</sup>
	1 <sup>st</sup> layer	2 <sup>nd</sup> layer			
1	13 (sigmoid)		1.6	38	0.95
	1 (rectified)		2.4	72	0.92
2	13 (sigmoid)	13 (rectified)	1.6	36	0.95
	11 (tanh)	11 (sigmoid)	1.5	36	0.96
	1 (rectified)	1 (sigmoid)	2.2	71	0.93

\* The results are just for illustration rather than listing all tested microscopic models.

Trips are formed by aggregating the continuous 1Hz data with equal time durations of 5, 15, 30, 60-minute. Each 1Hz record contained the actual and predicted fuel consumption from our microscopic model. For each trip, the fuel consumption over the 5, 15, 30, 60-minute durations was aggregated over actual/predicted values and compared to obtain the absolute percentage error of the prediction. Figure 7 presents a boxplot of the absolute percentage error (%) for the microscopic model at aggregated levels. It shows that when fuel predictions are aggregated between 5 to 60 minutes, the mean absolute percentage error reduces as the trip duration increases. However, the MAPEs were near or below 2%, which demonstrated the capability of the microscopic model to predict 1Hz fuel consumption rates and achieve high accuracy at 5 to 60-minute trip levels.

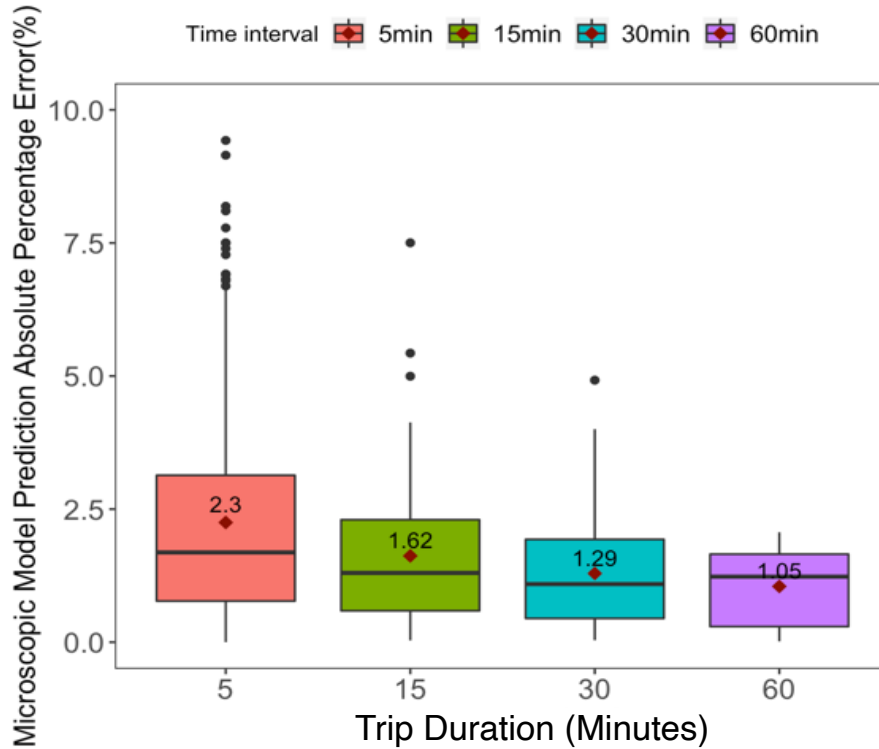
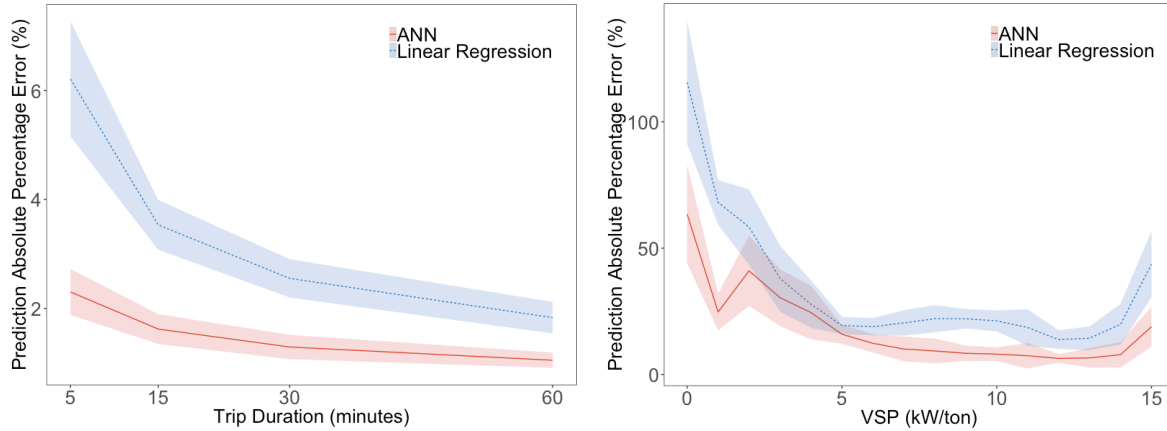


Figure 7. Boxplot of absolute percentage error for microscopic model predictions aggregated at 5, 15, 30, 60 minutes. The bar within each box represents the median absolute percentage error and the two sides of box correspond to 1<sup>st</sup> and 3<sup>rd</sup> quartiles. The diamond (with number) in a box is the mean value.

Figure 8 compares the absolute percentage prediction error for the ANN model and the non-neural network linear regression model as a function of trip duration (left) and instantaneous vehicle specific power (right). For Figure 8 (right), the measured and predicted fuel consumption data at 1HZ were averaged based on each VSP bins from 0 to 15 kW/ton to report prediction error. The MAPE and confidence intervals of the ANN model were consistently lower than those of the linear regression model, although the differences seemed to diminish as the trip duration increased. Specifically, the MAPE of the ANN model was consistently near 2%, while it was reduced from 6% to 2% for the linear regression model when the trip duration increased from 5 to 60 minutes. This reduction was expected, as shorter trip durations typically constitute more dynamic traffic and driving conditions. Thus, the ANN model can capture changes in fuel consumption more effectively using complex model formats. When accounting for VSP, the ANN model outperformed the linear regression model in all of the VSP bins. The improvements in prediction error are significant in low VSP areas (VSP < 3 kW/ton) for the ANN model.



**Figure 8. Mean absolute percentage error and 95 percentage confidence intervals for predictions of artificial neural network (ANN) model and linear regression model with the same independent variables as a function of trip duration (left) and vehicle specific power (right).**

### 5.2. Mesoscopic model selection and prediction performance

The mesoscopic model predicts fuel rates over a time period based on aggregated traffic pattern factors. Different model configurations were compared to determine the best prediction model (Table 4). The best model yielded a MAPE of 8.9%,  $R^2$  of 0.91, and a MAE of 4.0 liters per 100 km. The prediction metrics were calculated by comparing predicted and actual fuel consumption per km of each 5-minute trip. The average fuel consumption rate was 45 liters per 100 km, i.e. 5.2 miles per gallon, which is consistent, in terms of magnitude, with the average fuel consumption rate for diesel hybrid buses reported by Clark et al. (2009).

**Table 4. Description of Mesoscopic Level ANNs Configuration Selection Process.**

Hidden layers	Neurons		MAE (liter/ 100 km)	MAPE (%)	$R^2$
	1 <sup>st</sup> layer	2 <sup>nd</sup> layer			
1	23 (tanh)		4.2	9.4	0.84
	6 (sigmoid)		4.0	8.9	0.91
	1 (rectified)		5.1	11.4	0.85
2	23 (rectified)	23 (sigmoid)	4.3	9.6	0.86
	1 (sigmoid)	1 (tanh)	5.7	12.6	0.79

Figure 9 (left) presents boxplots of absolute percentage error (%) for the mesoscopic model at 5, 15, 30, 60-minute trip durations. Similar to the microscopic model, the MAPE of the mesoscopic model generally decreases as the trip time increases; however, it remains flat when the trip time is greater than 30 minutes. Figure 9 (right) evaluates the prediction error as a function of speed for

each trip duration by differentiating trips by speed ranges of 1-40 kph and 40-80 kph for each trip duration. The former trips correspond to typical urban driving, while the latter trips represent a combination of driving under urban, arterial, and highway conditions. There are limited data points to develop robust statistics on travel with an average speed of 40+ kph for 30 and 60-minute trips. This lack of data is understandable, given that the average speed of a transit bus in the United States is 22 kph (Hughes-Cromwick, 2019). As a result, a limited number of 30 or 60-minute trips would achieve average speeds above 40 kph. The MAPEs of 40-80 kph trips were higher than those of trips below 40 kph for 5 and 15-minute trips. Thus, higher uncertainty exists when predicting fuel consumption at high speed driving, which normally consists of a combination of urban, arterial, and highway driving.

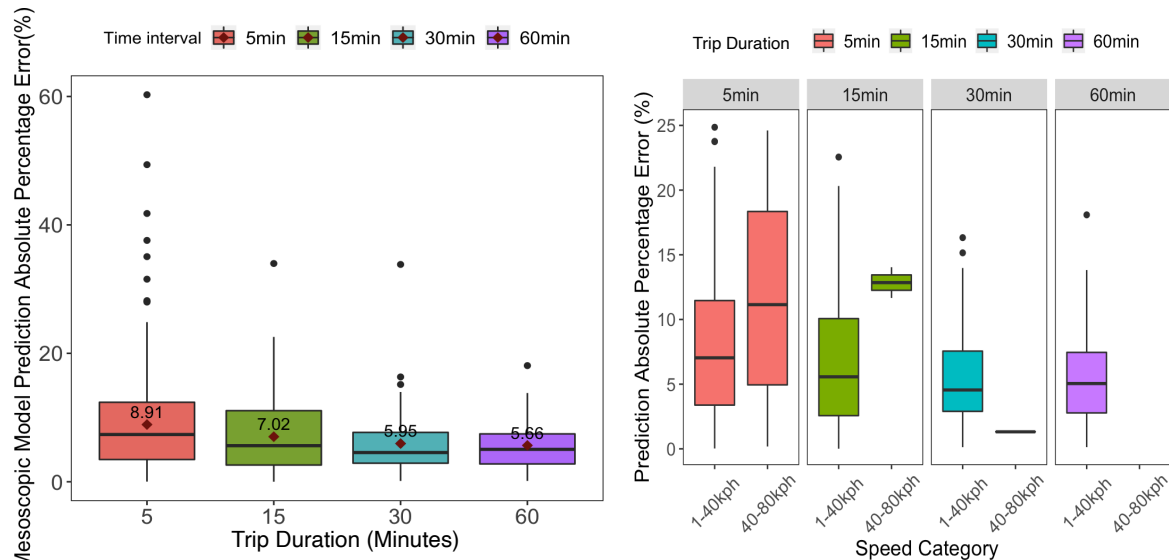


**Figure 9.** Boxplot of absolute percentage error for mesoscopic model predictions at 5, 15, 30, 60-minute trip duration (left) and discriminating by speed category (right). The bar within each box represents the absolute percentage error and the two sides of box correspond to 1<sup>st</sup> and 3<sup>rd</sup> quartiles. The diamond (with number) in a box is the mean value.

The mesoscopic model is based on eleven independent variables that are averaged at different trip durations to predict the fuel consumption rate of hybrid buses. Clearly, models with more input variables would result in stronger correlations with output variables and yield better prediction performance. However, due to challenges in data collection, the eleven variables may not be readily available. In this study, we explore the impacts of data availability on the performance of mesoscopic prediction models. First, three scenarios are established, which represented three levels of data availability. “Scenario 1” contained only the average speed variable, which is the minimum data requirement. This scenario is applicable because the average speed of a road

network is regularly monitored by transportation authorities. “Scenario 2” contained average speed and road grade variables. This scenario combines traffic data and infrastructure data that are normally available to transportation practitioners. “Scenario 3” contained the eleven independent variables. For each scenario, model selection procedure is conducted and the optimal model configuration is presented in Table 3. A higher MAPE was expected for scenarios with less input variables. The single input variable, Scenario 1, had a MAPE of 14%, which was the largest. Studies have used average speed as the sole piece of information to predict fuel consumption of vehicles, such as the Motor Vehicle Emission Simulator (US EPA, 2010) and Barth and Boriboonsomsin (2008). However, a few recent studies have adopted single input variable prediction models, due to concerns regarding prediction accuracy (Chen et al., 2017). The MAPE of the best model in Scenario 2 is 12%. The speed and road grade variables in Scenario 2 have been used in recent studies (Cuma and Koroglu, 2015; Sun et al., 2015; Zhang and E Yao, 2015). Specifically, speed and road grade can be used to calculate VSP, which is an effective proxy for vehicle power demand (Jimenez-Palacios, 1998).

**Table 3. Comparison of optimal ANN model configurations under different data availability scenarios.**

	Neurons		MAE (liter/100 km)	MAPE (%)	R <sup>2</sup>
	1 <sup>st</sup> layer	2 <sup>nd</sup> layer			
Scenario 1	2	--	6.3	14	0.77
Scenario 2	4	--	5.4	12	0.82
Scenario 3	6	--	4.0	8.9	0.91

Figure 10 compares the MAPE of fuel consumption estimates at 5, 15, 30, and 60-minute duration for the three scenarios in the mesoscopic and microscopic models. Within each scenario, it is observed that using data with longer trip durations led to improved prediction performance. This finding was expected because averaging longer time periods can reduce noise in data, which can improve prediction accuracy. However, averaging data into longer periods is not necessarily a better practice. The mean absolute percentage errors of the microscopic model were less than 2%. However, the extra effort to obtain detailed trajectory data must be balanced with improvements in prediction accuracy to justify the use of the microscopic model.

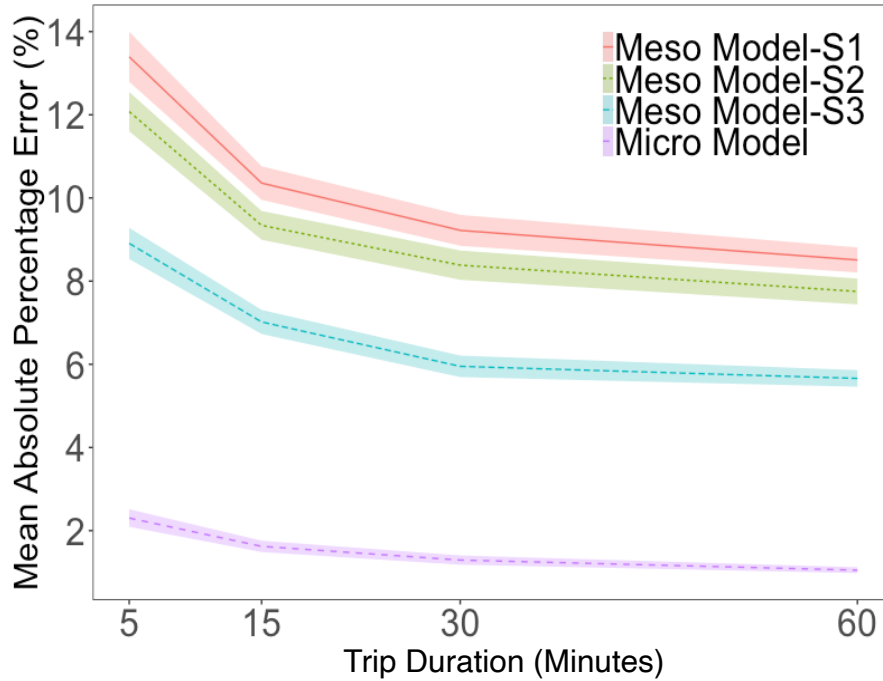


**Figure 10. Mean and 95 % confidence (shared area) absolute percentage error for microscopic and three scenarios of mesoscopic models as a function of trip duration.**

Relevant literature on fuel consumption estimation of transit buses are reviewed and their input variables and model setup are summarized in Table 4. Those models used input data at either 1Hz or trip-average granularity. The prediction outputs were liters per hour for 1Hz level prediction or trip-average fuel consumption rate (liters per kilometer). The input data (1Hz and 5-minute average granularity) from this study were applied to models from the literature to compare their prediction performances with our models. Table 4 summarizes the comparison results. The MAPEs of trip-level models from the literature ranged from 12% to 22%, which are consistent with the MAPEs reported in the literature using their data. The MAPEs of our models are between 5% to 8%. Three out of the four trip-level models in the literature utilized linear regression-based methods. The other models used the supporting vector machine (SVM) method and reported a MAPE of 12%. The two 1Hz microscopic models adopted quadratic and exponential regression methods and resulted in MAPEs of 47% and 59%, respectively, which were also aligned with results in their studies. If the 1Hz prediction results are aggregated into 5 to 60 minutes, their MAPEs are between 5% to 9%. The comparison shows the potential of the ANN model to accurately predict the fuel consumption of buses under real-world driving conditions.

**Table 4. Comparison with fuel consumption estimation models in literature.**

	Method type	Input variables	Granularity	MAPE
This study	ANN	Speed (average), acceleration, grade, temperature	Trip	5-8%
Frey et al. (2007)	Regression-Linear	VSP	Trip	12%
Delgado et al. (2011)	Regression-Linear	Speed (average), acceleration	Trip	22%
López-Martínez et al. (2017)	Regression-Linear	Speed (average, max), acceleration	Trip	18%
Zeng et al. (2015)	SVM	Speed (average, variance)	Trip	12%
This study	ANN	Speed, acceleration, grade, temperature,	1Hz	36% (1Hz) 1-2% (aggr. at 5-60 min)
Wang and Rakha (2016,2017)	Regression-quadratic	VSP	1Hz	47% 4-8% (aggr. at 5-60 min)
Hung et al. (2005)	Regression-Exponential	Speed	1Hz	59% 6-9% (aggr. at 5-60 min)

## 6 Conclusion

Hybrid buses have gained popularity in recent years due to their potential savings in transportation fuel. Estimating fuel consumption for hybrid diesel buses is challenging because its operation and driving conditions are diversified. In this paper, we proposed ANN microscopic and mesoscopic models to estimate fuel consumption of hybrid diesel buses based on long-term transit bus monitoring data collected from CARTA. The microscopic model predicted instantaneous fuel consumption rates based on driving, grade, and environment variables at the same frequency. The ANN-based microscopic model results showed 1-2% of cumulative absolute error when aggregating second level results to 5 to 60-minute trips. The results showed that ANN models can achieve lower error, compared to linear regression models, using with the same input variables. The mesoscopic model predicted average fuel rates for 5 to 60-minute trip durations based on traffic factors for the same period. Our results show that the absolute prediction error for mesoscopic models ranged between 5 and 9%. This range is higher than that of the microscopic model; however, the independent variables of the mesoscopic model, e.g. average traffic speed, congestion level, etc., are typically monitored by local transportation authority. The experimental data contained 1Hz data of hybrid and diesel buses that have similar driving conditions in terms of speed, engine demand, and road grade. Our investigation of fuel rate showed that hybrid buses have the largest fuel savings during low speed driving with high acceleration and none or increased

fuel consumption during highway driving. The electric motor of hybrid buses normally engages to supplement or replace a portion of propulsion provided by the diesel engine at low speed driving with high acceleration, which can help achieve better fuel efficiency. Similar fuel savings were observed in hybrid passenger car experiments that can be found in the literature. One limitation of this study is that the experiment did not collect operational data for electric motors within the hybrid bus. Therefore, we could not fully understand the energy management system mechanism within the hybrid bus. One future research direction may be to collect and leverage electric motor operation data from hybrid buses to better understand their fuel saving mechanism. Another future research direction may be to collect passenger load information on buses and assess the impacts of passenger load on the fuel consumption of hybrid buses under real world driving conditions.

### **Acknowledgements**

This material is based upon work supported by the Department of Energy, Office of Energy Efficiency and Renewable Energy (EERE), under Award Number DE-EE0008467. The views and opinions of authors expressed herein do not necessarily state or reflect those of the United States Government or any agency thereof. Specifically, neither the United States Government nor any agency thereof, nor any of their employees, makes any warranty, express or implied, or assumes any legal liability or responsibility for the accuracy, completeness, or usefulness of any information, apparatus, product, or process disclosed, or represents that its use would not infringe privately owned rights. Reference herein to any specific commercial product, process, or service by trade name, trademark, manufacturer, or otherwise does not necessarily constitute or imply its endorsement, recommendation, or favoring by the United States Government or any agency thereof.

## References

- Barth, M., Boriboonsomsin, K., 2008. Real-world carbon dioxide impacts of traffic congestion HEV fuel consumption. *Transp. Res. Rec.* 163–171. <https://doi.org/10.3141/2058-20>
- Beaudoin, J., Farzin, Y., Lawell, C., 2015. Public transit investment and sustainable transportation: A review of studies of transit's impact on traffic congestion and air quality HEV fuel consumption. *Res. Transp. Econ.* 52, 15–22.
- Bureau of Transportation Statistics, 2018. *Transportation Economic Trends 2018*. Washington, D.C. <https://doi.org/https://doi.org/10.21949/1502599>
- CARTA, 2020. *Chattanooga Area Regional Transportation Authority System Map*.
- Chen, Y., Zhu, L., Gonder, J., Young, S., Walkowicz, K., 2017. Data-driven fuel consumption estimation: A multivariate adaptive regression spline approach HEV fuel consumption. *Transp. Res. Part C Emerg. Technol.* 83, 134–145.
- Choi, H., Frey, H., 2010. Method for In-Use Measurement and Evaluation of the Activity, Fuel Use, Electricity Use, and Emissions of a Plug-In Hybrid Diesel-Electric School Bus. *Environ. Sci. Technol.* 44, 3601–3607. <https://doi.org/10.1021/es903330k>
- Cuma, M., Koroglu, T., 2015. A comprehensive review on estimation strategies used in hybrid and battery electric vehicles HEV fuel consumption. *Renew. Sustain. Energy Rev.* 517–531.
- Delgado, O.F., Clark & Gregory, N.N., Thompson, J.J., 2011. Modeling Transit Bus Fuel Consumption on the Basis of Cycle Properties. *J. Air Waste Manage. Assoc.* 61, 443–452. <https://doi.org/10.3155/1047-3289.61.4.443>
- Department of Energy, 2019. *Transit Buses by Fuel Type in United States*.
- Silva, J.D., Moura, F., Garcia, B., Vargas, R., 2015. Influential vectors in fuel consumption by an urban bus operator: Bus route, driver behavior or vehicle type? HEV fuel consumption. *Transp. Res. Part D Transp. Environ.* 38, 94–104.
- Frey, H., Roupail, N., Zhai, H., Farias, T., Gonçalves, G.A., 2007. Comparing real-world fuel consumption for diesel-and hydrogen-fueled transit buses and implication for emissions HEV fuel consumption. *Transp. Res. Part D Transp. Environ.* 12, 281–291.
- Frey, H.C., 2018. Trends in onroad transportation energy and emissions. *J. Air Waste Manage. Assoc.* 68, 514–563. <https://doi.org/10.1080/10962247.2018.1454357>
- Hassoun, M.H., 1995. *Fundamentals of artificial neural networks*. MIT press.
- Hofman, T., Van Druten, R., 2004. Energy analysis of hybrid vehicle powertrains, in: *Proc. IEEE Int. Symp. Veh. Power Propulsion*. pp. 1–8.
- Holmén, B.A., Sentoff, K.M., 2015. Hybrid-Electric Passenger Car Carbon Dioxide and Fuel Consumption Benefits Based on Real-World Driving. *Environ. Sci. Technol.* 49, 10199–10208. <https://doi.org/10.1021/acs.est.5b01203>
- Hughes-Cromwick, M., 2019. *2019 Public Transportation Fact Book HEV fuel consumption*.
- Hung, W.T., Tong, H.Y., Cheung, C.S., 2005. A modal approach to vehicular emissions and fuel consumption model development. 10, 1431–1440.
- Jimenez-Palacios, J., 1998. *Understanding and quantifying motor vehicle emissions with vehicle specific power and TILDAS remote sensing*. Massachusetts Institute of Technology.
- Karsoliya, S., 2012. Approximating Number of Hidden layer neurons in Multiple Hidden Layer BPNN Architecture. *Int. J. Eng. Trends Technol.* 3, 714–717.
- Lajunen, A., 2014. Energy consumption and cost-benefit analysis of hybrid and electric city buses. *Transp. Res. Part C Emerg. Technol.* 38, 1–15.
- Liu, L., Kotz, A., Salapaka, A., Miller, E. and Northrop, W.F., 2019. Impact of time-varying passenger loading on conventional and electrified transit bus energy consumption. *Transportation Research Record*, 2673(10), pp.632-640.
- López-Martínez, J., Jiménez, F., Páez-Ayuso, F., Flores-Holgado, M.N., Arenas, A.N., Arenas-Ramirez, B., Aparicio-Izquierdo, F., 2017. Modelling the fuel consumption and pollutant emissions of the urban bus fleet of the city of Madrid HEV fuel consumption. *Transp. Res. Part D Transp. Environ.*

52, 112–127.

- Maier, H., Dandy, G., 2001. Neural network based modelling of environmental variables: a systematic approach HEV fuel consumption. *Math. Comput. Model.* 33, 669–682.
- Clark, N., Zhen, F., Wayne, S., Schiavone, J., Chambers, Cl., Golub, A., 2009. Assessment of Hybrid-Electric Transit Bus Technology. Washington, DC: The National Academies of Sciences, Engineering, and Medicine
- Qi, X., Wu, G., Boriboonsomsin, K., Barth, M.J., 2016. Development and evaluation of an evolutionary algorithm-based online energy management system for plug-in hybrid electric vehicles HEV fuel consumption. *IEEE Trans. Intell. Transp. Syst.* 18, 2181–2191.
- Rogers, L.L., Dowla, F.U., 1994. Optimization of groundwater remediation using artificial neural networks with parallel solute transport modeling. *Water Resour. Res.* 30, 457–481.  
<https://doi.org/10.1029/93WR01494>
- Shen, Y., Zhang, H., Zhao, J., 2018. Integrating shared autonomous vehicle in public transportation system: A supply-side simulation of the first-mile service in Singapore HEV fuel consumption. *Transp. Res. Part A Policy Pract.* 113, 125–136.
- Sun, Z., Hao, P., Ban, X., Yang, D., 2015. Trajectory-based vehicle energy/emissions estimation for signalized arterials using mobile sensing data HEV fuel consumption. *Transp. Res. Part D Transp. Environ.* 27–40.
- Tang, X., Zhu, Y., Xu, L., 2016. The Analysis of Space-time Characteristics of Bus Operation and Energy Consumption Based on ArcGIS. *Energy Procedia* 104, 456–461.  
<https://doi.org/10.1016/j.egypro.2016.12.077>
- Taylor, B., 2006. Methods and procedures for the verification and validation of artificial neural networks HEV fuel consumption. Springer Science & Business Media.
- Taymaz, I., Benli, M., 2014. Emissions and fuel economy for a hybrid vehicle. *Fuel* 115, 812–817.  
<https://doi.org/10.1016/j.fuel.2013.04.045>
- Tennessee State Government, Tennessee Base Mapping Program, Elevation LiDAR.  
<https://www.tn.gov/finance/sts-gis/gis/gis-projects/gis-projects-elevation.html>, accessed on July 13<sup>th</sup>, 2020.
- US EPA, 2010. Motor vehicle emission simulator (MOVES): User guide for MOVES2010b.
- Wang, C., Ye, Z., Yu, Y., Gong, W., 2018. Estimation of bus emission models for different fuel types of buses under real conditions HEV fuel consumption. *Sci. Total Environ.* 640, 965–972.
- Wang, J., Rakha, H., 2016. Fuel consumption model for conventional diesel buses. *Appl. Energy* 170, 394–402.
- Wang, J., Rakha, H.A., 2017. Convex Fuel Consumption Model for Diesel and Hybrid Buses. *Transp. Res. Rec.* 2647, 50–60. <https://doi.org/10.3141/2647-07>
- Wayne, W., Clark, N., Nine, R., Elefante, D., 2004. A comparison of emissions and fuel economy from hybrid-electric and conventional-drive transit buses HEV fuel consumption. *Energy & fuels* 18, 257–270.
- White, P.R., 2016. Public transport: its planning, management and operation. Taylor & Francis.
- Wu, G., Boriboonsomsin, K., Barth, M.J., 2014. Development and evaluation of an intelligent energy-management strategy for plug-in hybrid electric vehicles HEV fuel consumption. *IEEE Trans. Intell. Transp. Syst.* 15, 1091–1100.
- Wu, X., Zhang, S., Wu, Y., Li, Z., Zhou, Y., Fu, L., Hao, J., 2015. Real-world emissions and fuel consumption of diesel buses and trucks in Macao: From on-road measurement to policy implications HEV fuel consumption. *Atmos. Environ.* 120, 393–403.
- Wu, Y., Song, G., 2013. Feasibility study of fuel consumption prediction model by integrating vehicle-specific power and controller area network bus technology HEV fuel consumption. *Transp. Res. Rec. J. Transp. Res.* 2341, 66–75. <https://doi.org/10.3141/2341-07>
- Xu, Y., Li, H., Liu, H., Rodgers, M., Guensler, R., 2017. Eco-driving for transit: An effective strategy to conserve fuel and emissions HEV fuel consumption. *Appl. Energy* 194, 784–797.

- Zeng, W., Miwa, T., Morikawa, T., 2015. Exploring Trip Fuel Consumption by Machine Learning from GPS and CAN Bus Data, *Journal of the Eastern Asia Society for Transportation Studies*.
- Zhang, R., E Yao, 2015. Electric vehicles' energy consumption estimation with real driving condition data HEV fuel consumption. *Transp. Res. Part D Transp. Environ.* 41, 177–187.
- Zhang, S., Wu, Y., Liu, H., Huang, R., Yang, L., Li, Z., Fu, L., Hao, J., 2014. Real-world fuel consumption and CO2 emissions of urban public buses in Beijing HEV fuel consumption. *Appl. Energy* 113, 1645–1655.